PHYSICAL ACOUSTICS

Physical acoustics deals with the principles of high-frequency sound and related phenomena, as well as their applications

to basic research in physics, chemical physics, and biophysics. Physical acoustics has a wide scope, including problems of wave propagation (i.e., reflection, refraction, transmission, scattering, diffraction, interference, and resonance or mode conversion, of which the essential part is in common with optics); mechanisms of generating and receiving sound waves; and linear and nonlinear interactions with light, electric, magnetic, or stress fields in the medium. Coupling with microscopic structures of matter in a static or a dynamic manner is also an important subject and provides fundamental knowledge for studies of materials science by sound waves. In contrast to general acoustics, which treats only the audible sound in air, any material can be the medium in physical acoustics: for example, crystal, metal, amorphous, ceramic and composite, liquid and solutions, liquid crystal, biological substances, and gas. In many cases, the frequency is in the ultrasonic range, and the longitudinal, transverse, and other vibration modes are considered as sound waves. Physical acoustics is the basis for all industrial, medical, and underwater applications of ultrasound.

HISTORY

While the history of acoustics can be traced back to the age of Pythagoras, physical acoustics in a modern sense started in the seventeenth century when Galileo introduced correct facts about sound frequency and wavelength in his "Dialogues Concerning Two New Sciences" (1). Physicists in the eighteenth century, including Newton, Euler, and Laplace, developed theories of sound propagation (Newton's equation of sound velocity in air was somewhat strange), and the outline of physical acoustics was established by Rayleigh in his celebrated "Theory of Sound" at the end of nineteenth century. Sound with frequency beyond the audible limit also was studied in those days. Savart generated frequencies up to 24 kHz with a toothed wheel and an elastic plate, and Galton invented a whistle that achieved 80 kHz. Savart and Galton conducted auditory tests on humans and animals.

In the early twentieth century, there was a breakthrough in the modern age of physical acoustics. Spurred by urgent demand for underwater detection stimulated by the *Titanic* disaster and the submarine menace in World War I, in 1917 Langevin invented a piezoelectric quartz oscillator that produced ultrasonic waves of controlled frequency and amplitude. The quartz transducer was immediately applied to the ultrasonic interferometer by Pierce, who studied the velocity dispersion and absorption in CO_2 gas and launched molecular acoustics, an important branch of physical acoustics. Wood and Loomis demonstrated the physical, chemical, and biological effects of high-intensity ultrasound generated with a large quartz plate. As for the optical effects of sound, which had been known since the 1800s, Brillouin proposed a basic theory of light diffraction in 1922, and experiments were conducted in water and transparent solids soon after. The invention of the laser in the 1960s was an encounter of two coherent waves; the ideal light source led to the breakthrough of acousto-optics, with brilliant applications both in the laboratory and industry. The progress of ultrasonics kept pace with the progress of electronics. Cady incorporated a quartz oscillator in the vacuum tube circuit in 1920; the oscillator showed remarkably stable oscillation. The electric pulse technique originally developed for radar systems during World War II was soon introduced to ultrasonics and magnified the potential of ultrasound on a large scale. Physical acoustics today owes much to these modern developments of ultrasonics, electronics, and optics.

ULTRASOUND

Ultrasound involves sound or mechanical vibration with frequencies higher than 20 kHz (16 kHz in some countries). Because this term was originally used with reference to the frequency range beyond human audibility and because the audible limit depends much on the individual and on age, the boundary is arbitrary and this definition is a nominal one made for the sake of convenience. While most practical applications are at frequencies up to several tens of megahertz, ultrasonic waves for scientific purposes extend over a much wider range: Hypersonic frequency above 1 GHz is commonly used in molecular acoustics or in studies of condensed matter; and pretersonic radiation ($\sim$100 GHz) is used in low-temperature physics. The upper limit of ultrasonic frequency is not explicitly defined. At such a high frequency range, where the wavelength is comparable to the molecular mean free path or the interatomic distance, the medium can no longer be considered an elastic continuum. In this sense, 1 THz is the limiting frequency in principle.

Ultrasonic Velocity

Sound waves propagate with a kind of dynamic balance between the inertia of mass and the elastic restoring force, and the velocity is generally given as $v = \sqrt{E/\rho}$, where ρ is the density and E is the adiabatic modulus of elasticity appropriate for the sound mode. In ideal gas, this equation is simply reduced to $v = \sqrt{\gamma RT/M}$ with the aid of thermodynamics, where γ is the specific-heat ratio, R the gas constant, and M the molecular weight. The velocity depends only on T (not on pressure) and can be used for temperature measurement. Of the three states of matter, gas has the lowest longitudinal velocity, ranging from 200 to 400 m/s with the exceptions of hydrogen (1707 m/s) and helium (997 m/s). The moduli for longitudinal and transverse modes are $K + 4/3G$ and G, respectively, where K is the bulk modulus for hydrostatic volume change and G the shear modulus. In liquid, $G = 0$ with very rare exceptions and only longitudinal waves propagate whose velocity is roughly between 1000 m/s and 2000 m/s (the transverse waves travel but a very short distance in a highly viscous liquid). On the other hand, solids exhibit much more complicated features (2). In an isotropic medium with infinite extension, longitudinal and doubly degenerated transverse waves propagate, the former having a velocity roughly twice as high as the latter. Anisotropic media such as crystal or composites have three independent modes that differ in velocity. In many cases, they are quasi-longitudinal and quasi-transverse modes whose wave vector is pointed off the direction of propagation. Waves in a medium with boundaries are also of interest (3). The Rayleigh mode appears on the surface of a semi-infinite solid, is usually referred to as a surface acoustic wave (SAW), and has important applications in electronics devices. Lamb waves propagating in the plane of

elastic plates have many modes of different orders depending on the ratio of the thickness to the wavelength. Generally speaking, ultrasonic waves have a linear relation between ω, the angular frequency, and k, the wave number: The phase velocity defined as ω/k is a constant. There are cases, however, in which the velocity depends on frequency. Such velocity dispersion appears in a medium with boundaries, as is the case in Lamb waves, or in a medium involved in relaxation phenomena (described in the section entitled Molecular Acoustics).

Characteristic Features of Ultrasound and Its Applications

There are two aspects of ultrasonic waves: one as high-frequency carrier waves and the other associated with a high-energy concentration of elastic vibration. Regarding the former, ultrasound has a great advantage under water, where electromagnetic waves are hardly of use. There are many applications, including sonar, depth meter, and ocean tomography. Nondestructive evaluation of opaque substances, such as in defect detection or imaging, is also an important application of ultrasound as carrier waves. Ultrasonic diagnosis is preferred because of its relatively weak influence on the human body in comparison with X rays. In the field of modern electronics, ultrasound has found a variety of new applications, such as SAW filters, delay lines, light modulators, frequency control devices, and sensors for various purposes. Power ultrasonics is the use of vibration intensities for creating irreversible changes of materials and has widespread applications. Cleaning, welding, drilling, cutting, material processing, emulsification, and atomization of liquids with ultrasonic vibration are standard techniques in industry; and vibrating surgical tools are commonly used in hospitals. Most of the applications in sonochemistry, such as polymerization, cutting of polymer chains, and promotion of reactions with ultrasound, take advantage of ultrasound's energy concentration.

Ultrasonic Transduction

A common technique to generate ultrasonic waves is based on piezoelectricity (4). A plate of piezoelectric material with electrodes on both faces converts electric oscillation into elastic vibration and emits ultrasonic waves into a medium in direct contact with it. Piezoelectric transducers of different materials and types are available; the most suitable one is chosen depending on the frequency range and the kind of medium. Piezoelectric ceramics such as PZT are currently used for all purposes over the range of 10 kHz to 10 MHz. Quartz is preferred in laboratories for its high Q factor and stability over the range from 1 MHz to 1 GHz. Thin films of zinc oxide or cadmium sulfide sputtered on a substrate of sapphire or fused quartz are effective in the hypersonic range (5). The piezoelectric polymer polyvinylidene fluoride (PVDF) is a flexible film that fits curved surfaces. These ultrasonic transducers are used for receiving signals as well.

PHONON

While ultrasound is a macroscopic vibration in an elastic continuum, the phonon is a quantum concept of microscopic vibration in an atomic lattice that was originally introduced in describing the heat capacity of solids at low temperatures (6). Thermal energy drives a collective motion of atoms interconnected with elastic force and excites the lattice vibration around their equilibrium positions, which propagates as a phonon with a certain frequency and wavelength. When the wavelength is much longer than the lattice constant (interatomic distance), the phonon is regarded as ultrasound in a continuum with a linear dispersion relation between ω and k. In the frequency range above terahertz, where one wavelength includes only a few atoms, the lattice dynamics are better understood with the concept of the phonon. The dispersion curve shows a strong nonlinearity reflecting the discrete nature of the lattice. In the simplest lattice of identical atoms, for example, the group velocity defined as $d\omega/dk$ decreases with k and perfectly vanishes at $k = \pi/d$, as shown in Fig. 1, where d is the lattice constant. This is the limiting wave number: The wavelength is just twice the lattice constant and the phonon loses its meaning as propagating waves. The dispersion relation can be derived within the framework of classical theory by solving the equation of motion for the chain of atoms. The curve generally has three branches representing three independent phonon modes associated with the longitudinal and the two transverse modes of ultrasound. In quantum theory, each phonon has energy $\hbar\omega$ and behaves as a particle with momentum $\hbar k$ in perfect analogy with the photon, the energy quantum of light. The vibration energy of the lattice can take only those discrete levels with intervals $\hbar\omega$ and is considered to be a collection of n phonons as $n\hbar\omega$ (the ground-level energy $1/2\hbar\omega$ is added more strictly). An increase in the vibration amplitude in a classical sense is an increase in n, the quantum number. This quantum description is very important in dealing with problems such as heat conduction in dielectric solids, electric conductivity in pure metals, and Brillouin scattering in transparent media. These phenomena are interpreted in terms of interparticle collisions—phonon–phonon, phonon–electron, and phonon–photon, respectively.

Originally developed for crystals, the concept of the phonon is expanded to other substances, amorphous, liquid, or gas: The phonon is an energy quantum of local elastic vibration excited by thermal energy.

Thermal and Electric Conduction

Any substance at a finite temperature is considered a container crowded with phonon particles. A local increase in tem-

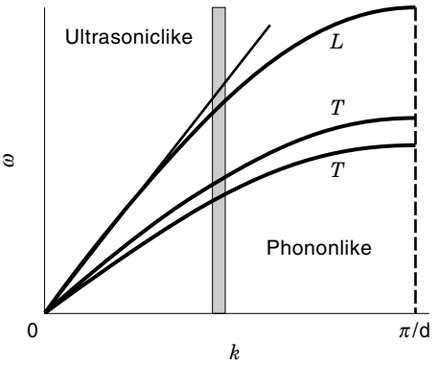

Figure 1. Dispersion of longitudinal and two transversal modes of phonon in lattice.

perature means a local increase in n, and the natural preference for equilibrium drives some of the phonons out of the heated region. Free flight of the phonon at its own group velocity is immediately intercepted by other phonons, however, and the successive collisions give rise to multiple scattering. (The phonon-phonon interaction occurs through the anharmonic term in the interatomic potential.) Here is the image of phonon diffusion, leading to a good analogy with gas kinetics, in which molecules collide with each other and diffuse. The thermal conductivity is then given by the familiar equation common to various transport phenomena: $\kappa = (1/3)Cvl$, where l is the phonon mean free path (mean distance between successive collisions) and C is the heat capacity of the lattice per unit volume. At room temperature, l is on the order of nanometers, while $d = 0.1$ nm.

In metals, free electrons have a major role in thermal conduction as well as in electric conduction, in which phonons have significant influence (7). Phonon-electron collisions are the dominant cause of resistance in metals that have few structural imperfections (impurities, dislocations, and point defects), and the resistivity decreases rapidly as the phonon population decreases at low temperatures. In metals in a superconducting state, on the other hand, phonons have a positive effect on electron conduction. Superconductivity is theoretically explained by the electron pairs, and such pairing occurs because the phonon-electron interactions induce an attractive force between two electrons, and the force exceeds the normal coulomb repulsive force below the critical temperature.

Phonon Imaging

At very low temperatures, where l has a macroscopic length of 1 mm or longer, phonon propagation becomes rather ballistic than diffusive, as is observed by the experiment with a heat pulse. A very short laser pulse strikes a single crystal immersed in liquid helium and instantaneously heats the surface coated with a metal film. The heat pulse excites phonons, which fly through the crystal toward the opposite surface and are detected with the bolometer of a superconducting device. The signal typically has three peaks arriving at different times, which are assigned to the three phonon modes, and the delay time determines the group velocity of each mode. More interesting is phonon imaging (8). The anisotropic group velocity inherent in the crystal deflects the phonon orbit, which otherwise would be straight, and the deflection depends on the direction of flight. Consequently, the phonons arriving at the detection surface are far from uniform; they are focused and dense at some positions while sparse at others. The phonon distribution thus exhibits a pattern characteristic to crystal symmetry. In the experiment, the role of the exciter and the detector are exchanged without any significant difference: The bolometer is fixed and, instead, the laser spot scans over the exciting surface in a raster manner (TV scan). The two-dimensional display of the detected signal gives the phonon image as shown in Fig. 2.

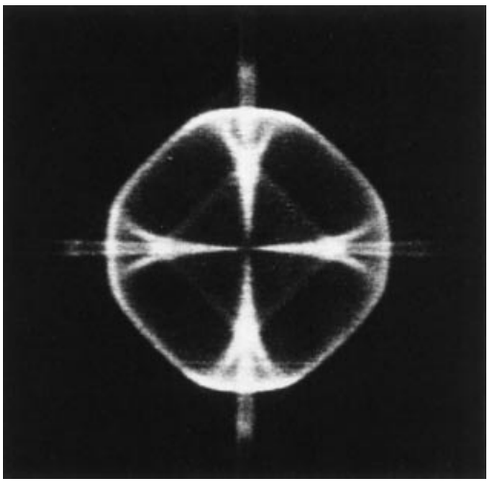

Figure 2. High-resolution phonon image for the (100) surface of silicon crystal. After Tamura, Shields, and Wolfe (8).

INTERACTION BETWEEN SOUND AND LIGHT

There are generally two effects, sound on light and light on sound, which are referred to as acousto-optics (9) and photoacoustics (10), respectively. In the former, sound waves give a periodic change to the refractive index of the medium, and the light passing through the area is modulated spatially and temporally. On the other hand, photoacoustics is the generation of sound by light: The optical energy is dissipated into heat, and the local expansion in the medium propagates as elastic waves. There is also a case in which the electric field of light directly introduces strain through the electrostrictive effect (the second-order effect of strain proportional to the square of the electric field and common to all dielectric materials).

Acousto-optics

Three phenomena of the same origin, yet apparently different, are observed depending on the sound frequency. Light deflection occurs in the range below ~1 MHz, as shown in Fig. 3(a). Sound waves with a long wavelength cause an index

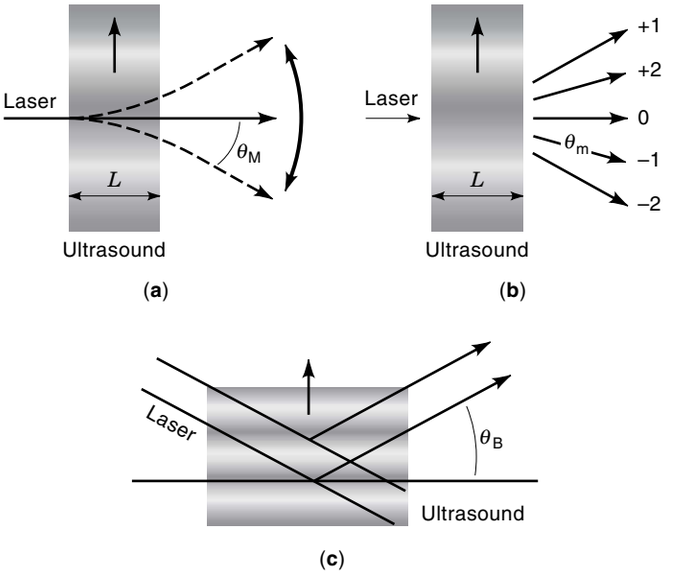

Figure 3. Three phenomena of acousto-optics: (a) Beam deflection at $f \leq 1$ MHz, (b) Raman-Nath diffraction at a few megahertz, and (c) Bragg reflection at $f \geq 50$ MHz.

gradient that deflects a narrow beam (usually laser) crossing the sound, as understood in geometrical optics. Since the gradient changes from negative through zero to positive with the phase advance, the light beam moves to and fro at the sound frequency. The sound oscillation is expressed as an alternating change in the refractive index from its average value n_0 as $n(t) = n_0 + \delta n \sin \omega t$, where δn is the amplitude of the refractive index. Under a low-amplitude assumption that the light trajectory is approximated with an arc, the deflection angle θ after the sound beam with width L is given by $\sin \theta(t) = (kL/2)\, \delta n \sin \omega t$. This assumption holds at $kL\sqrt{\delta n/n_0} \leq 1$. The deflection phenomenon provides absolute measurement of sound pressure amplitude P_0. The maximum angle of deflection θ_M gives P_0 as $\sin \theta_M = (kL/2)(dn/dP)P_0$, where (dn/dP) is a material constant and 1.47×10^{-10} Pa^{-1} in water.

In the intermediate region from 1 MHz to ~10 MHz, Raman-Nath diffraction is observed, as shown in Fig. 3(b). The periodical dense and sparse regions in the medium work as a phase grating, which modulates the plane waves into sinusoidal wave fronts, and diffraction of several orders appears in the far field. The intensity of the mth-order diffraction is given by

$$I_m = I_i J_m^2(r) \tag{1}$$

where I_i is the incident intensity and $J_m(r)$ is the mth-order Bessel function. The argument r is termed the Raman-Nath parameter and is written as $r = qL\ \delta n$, with q being the light wave number in the medium. The angle of the mth-order light is given by $\sin \theta_m = mk/q$, where θ_m is the value in the medium. The grating running at the speed of sound imparts a frequency shift of mf to the mth diffracted because of light, where $f = \omega/2\pi$ is the sound frequency. Since $J_1^2(r)$ is proportional to r^2 at $r < 1$, this phenomenon is used for optical detection of ultrasonic waves.

At frequencies higher than ~50 MHz, Bragg reflection occurs, as shown in Fig. 3(c), which is analogous to X-ray diffraction in crystals. Light is reflected by sound wave fronts if the angle of incidence satisfies the following equation of Bragg's condition:

$$2q \sin \theta_B = k \tag{2}$$

where θ_B is the Bragg angle. The optical frequency is shifted up by f if the sound direction is against the light, as shown in the figure, and shifted down in the opposite configuration. Reflected intensity is given by

$$I = I_i \sin^2(r/2) \tag{3}$$

The acousto-optic light modulators have the advantage that total reflection occurs at $r = \pi$. The harmonic nature of sound gives rise only to first-order diffraction in contrast to X-ray diffraction, which causes many higher orders. The preceding description of acousto-optics is based on the simplest case of longitudinal waves in isotropic media. The transverse waves introduce an anisotropic index and rotate the polarization plane of light (i.e., a kind of photoelasticity occurs). In single crystals, the sound velocity and refractive index have an anisotropy that should be expressed in tensors, and the acousto-optic phenomena exhibit a complicated feature involving both longitudinal and transverse waves.

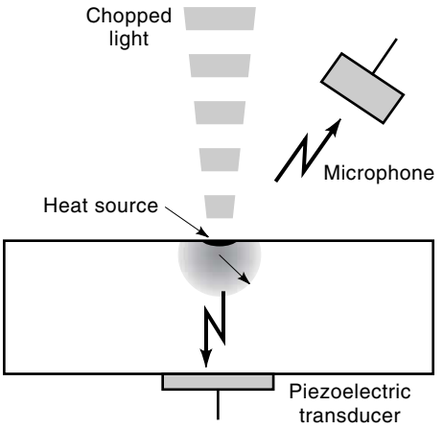

Figure 4. Generation and reception of photoacoustic signal in solid.

Photoacoustics

Light irradiation raises some degree of freedom in the medium to an excited state, which recovers the initial equilibrium through a radiative or nonradiative relaxation process; the latter is observed as photoacoustics (the former is photoluminescence). The light source chopped at f Hz (typically lower than 1 MHz) generates an acoustic signal, which reflects local properties for (1) light absorption, (2) heat generation, (3) thermal conduction, and (4) expansion. The principle of photoacoustics is shown in Fig. 4 for the case of solid samples. Heat generated by the light diffuses over a range of thermal diffusion lengths μ, determined by the chopping frequency as $\mu = \sqrt{\kappa/(\pi f \rho C)}$, where κ and C are the thermal conductivity and specific heat of the medium, respectively. The periodic expansion within the range of μ excites elastic waves at f, which propagate out of the range and are detected by a microphone in air, which picks up small pressure changes in a tight cell containing the specimen or a piezoelectric transducer bonded to the specimen. Information on microscopic structure or composition in the range of μ is obtained from the amplitude and phase of the acoustic signal. Two different types of experiment are usually conducted: photoacoustic microscopy (PAM) and photoacoustic spectroscopy (PAS). A focused laser spot scans the surface of the specimen in PAM, and the photoacoustic signal is used to form a magnified image of subsurface structure within the depth of μ, which affects any of the four aforementioned properties. Microcracks, voids, or fabricated structures hidden underneath appear in the image. At typical frequencies of 10 kHz to 1 MHz, μ is in the range from 50 to 5 μm, and information at different depths is available by varying f. Spatial resolution of PAM is determined by the larger of either the laser spot size or μ. In some cases, an electron beam is useful as an exciting source instead of the laser.

Light wavelength is swept from visible to infrared in PAS, and the photoacoustic signal is used for detection of absorption in spectroscopy. In addition to its high sensitivity, PAS has the advantage of observing the spectrum of opaque substances. Care should be taken, however, that PAS involves the preceding four properties, while standard spectroscopy observes only light absorption. Photoacoustics in the spectroscopic sense is very effective in detecting infinitesimal components in liquid and gas and is commonly used for checking air

pollution or the quality of super-pure water for semiconductor processes.

Since the origin of photoacoustics is the photothermal effect, direct observation of the heat produced is also useful. There are various techniques that detect, for example, infrared radiation, surface expansion with a laser Michelson interferometer, and beam deflection of a prove laser passing through air in close vicinity of the heated region. These techniques are usually included in photoacoustics in a wider sense, though they do not pertain to the acoustic signal.

VISUALIZATION OF THE SOUND FIELD

Visual observation of the ultrasonic field is sometimes very helpful in studying the various wave phenomena, and different techniques have been developed for this purpose. In the photographic method, a printing paper is put in a tank of diluted developer and ultrasonic waves normally illuminate the paper. The ultrasonic field promotes development and soon reveals its sectional distribution as a dark and bright pattern. This experiment can be conducted in a lighted room. Instead of the printing film, a black plastic plate coated with cholesteric liquid crystal can be used as the detector, which displays the intensity distribution in color. High-intensity ultrasound in water is directly seen for the accompanying sonoluminescence (11): The ultrasonic cavitations emit very weak visible light when they collapse at each cycle. A small amount of luminol in alkane solution strengthens the emission and the three-dimensional distribution can be seen with the naked eye. Propagation of CW (continuous wave) or pulse ultrasound is most clearly visualized by the Schlieren technique in liquids and by dynamic photoelasticity in transparent solids.

Schlieren Technique

The inhomogeneous refractive index in a transparent medium was visualized by Schlieren, whose principle is very simple. Light from a point source is once collimated with a lens, and another lens forms its real image on the focal plane. A glass plate with a black dot or a knife edge stops the light to produce a uniformly dark field of view. The medium is put between the two lenses, and the region of index gradient partially deflects the ray off the axis, and it emerges as a bright portion in the view field. This principle combined with Raman–Nath diffraction provides visualization of ultrasonic waves meeting at right angles to the light beam, as shown in Fig. 5. The second lens forms bright spots of different orders

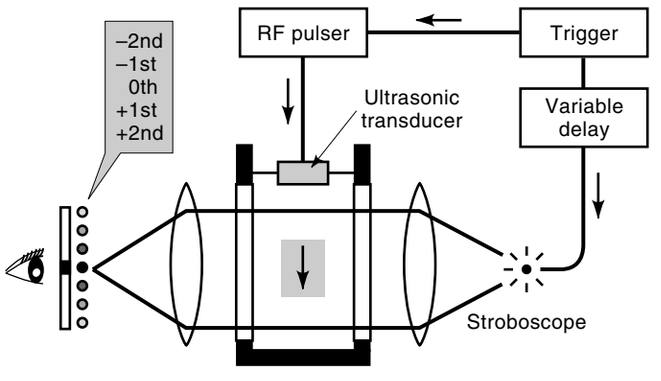

Figure 5. The stroboscopic Schlieren method provides a slow-motion picture of an ultrasonic pulse propagating in water.

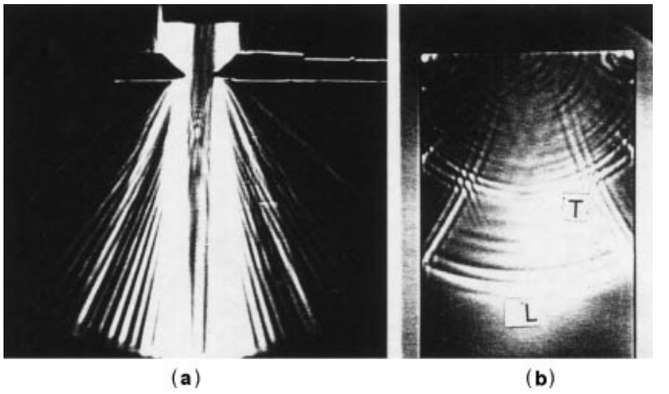

Figure 6. Ultrasonic pulse visualized by (a) stroboscopic Schlieren and (b) dynamic photoelasticity. In (a), a long pulse at 10 MHz has just passed through a slit with 3 mm width in water, showing a complicated diffraction pattern. Both longitudinal (L) and transversal (T) modes are simultaneously excited in (b) and propagate at different velocities in the glass block. The former is converted to the transversal mode at the side surfaces.

that align vertically on the focal plane. The 0th-order light is shut out and all the others observed by an eye or a camera reproduce the CW sound field.

Ultrasonic pulse is also visualized using a sharp stroboscope as the light source. The pulse is repeatedly generated and the light flashes every time after the pulse shot with a delay of a few μs when it comes into the light beam. While a still picture is obtained with a fixed delay, as shown in Fig. 6(a), a slow-motion picture of the running pulse is taken with a video camera by sweeping the delay time.

A variation of the Schlieren technique is the isochromat method, which uses a pinhole instead of the black dot and observes only first-order diffraction of a white light source (a Xenon lamp, for instance). As shown by Eq. (1), the first-order intensity depends not only on the sound amplitude but also on the light wavelength. Therefore, the visualized image has different colors that change from white through orange, violet, blue, green, to yellow as the amplitude at each point increases. The fine structure of the amplitude distribution is displayed as an isochromat graph, from which a quantitative estimate can be made.

Dynamic Photoelasticity

The Schlieren technique lacks sufficient sensitivity in solids due to their low compressibility, and birefringence induced by the sound waves is used for visualization instead (12). The experimental arrangement with a point light source and two lenses is similar to that of the Schlieren technique, except for a polarizer and $\lambda/4$ plate put before the medium and another $\lambda/4$ plate and analyzer behind it. The light passes through the medium as circularly polarized waves, and any change in polarization due to the waves is detected by the analyzer, whose axis is adjusted for highest contrast. This configuration is sensitive in all directions of propagation in the plane perpendicular to the optical axis, and both longitudinal and transversal waves are visualized. Note that the longitudinal mode has a component of shear strain that is four-thirds of the bulk strain and contributes to the photoelasticity. Figure 6(b) shows short pulses of longitudinal and transversal waves

in a glass block. A slow-motion picture is also available with the stroboscope and variable delay.

MEASUREMENT OF ULTRASONIC VELOCITY AND ABSORPTION

Many different techniques have been developed for measuring velocity and absorption, which are the fundamental quantities characterizing materials. The pulse method is most commonly used in laboratories and industry over a wide frequency range (13); the CW method includes the various types of resonance techniques and the ultrasonic interferometer (14); and the optical method is used at high frequencies for transparent liquids and solids. Accuracy higher than 0.1% is readily obtained for velocity measurements, while absorption measurement usually has a 5 to 20% error.

Pulse Method

The through-transmission type of pulse method has two piezoelectric transducers bonded to parallel surfaces of the solid block under study or attached to a cell for the liquid sample, as shown in Fig. 7. An ultrasonic pulse of $\sim 1\mu$s duration is injected into the specimen and multiply reflected between the two faces. The interval between the adjacent echoes in the received pulse-echo train gives $2t$, the round-trip time of the pulse, from which the velocity is obtained with the distance between the two transducers. There are a few techniques for the precise determination of t. In the pulse-echo-overlap method, the first and the second pulses are displayed on an oscilloscope. The trigger frequency is adjusted so that there is an overlap from cycle to cycle, and the period gives $2t$. In the sing-around method, the first pulse is gated out and triggers the next excitation of ultrasonic pulse. Thus the pulse runs around the loop of the acoustic and electric circuit, and t is obtained from the period. The period includes a delay in the electric circuit, however, and absolute measurement is difficult. This method is useful for automatic measurement of small changes in velocity.

Absorption measurement in liquid is made by increasing the distance x between the transducers, and attenuation in the pulse height, written as $\exp(-\alpha x)$, gives α, the absorption coefficient. At frequencies lower than 10 MHz, the sound diffraction causes an apparent loss that should be corrected theoretically. Above 100 MHz, on the other hand, parallelism between the two transducers is most important for accuracy. Absorption in a solid sample is obtained from decay in the echo train. Absolute measurement is difficult, however, since the reflection at the transducer/sample interface gives an additional loss.

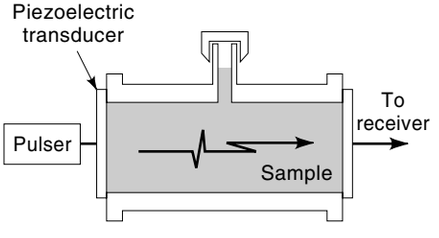

Figure 7. Sample cell of pulse method used for velocity measurement in liquid.

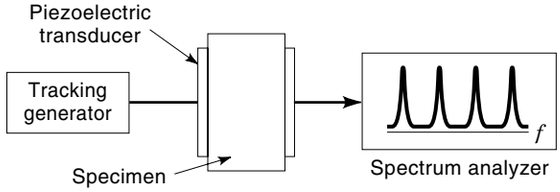

Figure 8. Resonance method for velocity and absorption measurement in solid.

The reflection type of pulse method has one transducer that works as a transmitter and a receiver. The pulse method has the advantages that the injected acoustic energy is low, on average, which otherwise would heat the specimen; and the crosstalk between the received signal and stray of the driving signal is avoided.

CW Method

Sound waves confined between two interfaces interfere and resonate when the distance equals half the wavelength multiplied by an integer. Figure 8 shows the principle of the resonance method used for a solid specimen. The driving frequency is swept and the resonance spectrum is observed. The peak interval Δf determines the velocity as $v = 2\Delta fd$, and the broadening δf gives the absorption as $\alpha = \pi\delta f/v$. For fear that the piezoelectric transducers affect the resonance, they are used below their own fundamental resonance where an even frequency response is expected. The resonance method is also used in liquid for absorption measurement in the megahertz range.

An ultrasonic interferometer is used for liquid or gas. The distance is swept instead of the frequency and the velocity is determined as $v = 2\Delta df$ from Δd, the interval in the resonance peak obtained as a function of d. The ratio of the peak to the bottom decreases as d increases, from which the absorption is obtained. In the correlation method, the received signal electrically interferes with the driving signal by a mixer, whose output reproduces the spatial decay of the ultrasonic waveform in the sweep of d.

Optical Method

The intensity of Bragg reflection given by Eq. (3) is proportional to the square of the ultrasonic amplitude (i.e., $I \propto \delta n^2$ at $r \ll 1$) and is used for optical detection of ultrasound. It has the advantage that the waves to be measured are hardly disturbed. Furthermore, Bragg's condition of Eq. (2) provides accurate measurement of the wave number by θ_B in the range above 1 GHz, where k has a value comparable to q. The high-resolution Bragg reflection (HRB) method useful in the UHF (ultrahigh frequency) range is based on the following principle (15): The spatial decay of ultrasonic amplitude is expressed as $\exp(-\alpha x)\sin k_0 x$. The Fourier transform of this equation gives the wave number spectrum of Lorentzian form written by

$$S(k) = 1/\{(1 + [(k - k_0)/\alpha]^2\} \tag{4}$$

The spectrum has a peak at $k_0 = \omega/v$ and a width of α. Hence, the Bragg angle for spatially decaying waves has a distribution centered at θ_0 and with a width $\Delta\theta$, and one gets $v =$

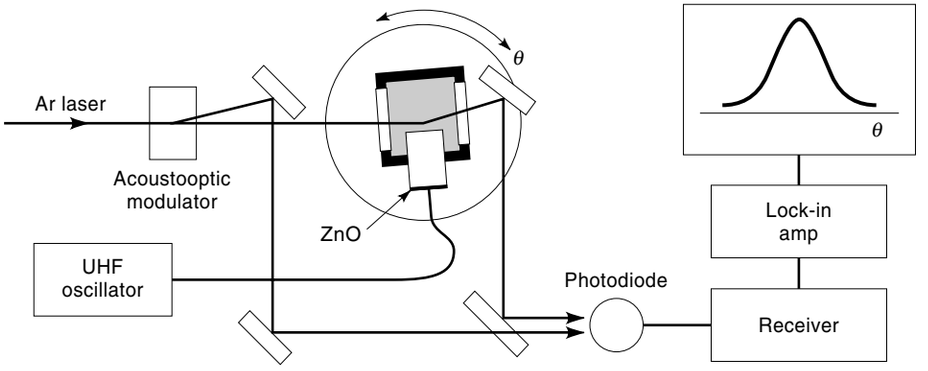

Figure 9. High-resolution Bragg reflection (HRB) method for velocity and absorption measurement in the UHF range.

$\omega/(2q \sin \theta_0)$ and $\alpha = 2q\Delta\theta \cos \theta_0$ from Eqs. (2) and (4). Figure 9 shows a block diagram of the HRB method for liquid specimens. A ZnO piezoelectric film excites continuous waves in the liquid where the laser is incident, and the reflected light is observed as sweeping the angle of incidence around θ_0. Figure 10 shows an example of the k spectrum obtained at 1.5 GHz as a function of θ, from which velocity and absorption are determined. The optical heterodyne detection gives high sensitivity and sufficient angular resolution.

Brillouin Scattering

Measurement of velocity and absorption generally requires artificial excitation of ultrasound; one exception is Brillouin scattering (16). Every substance has spontaneous phonons of thermal origin propagating in all directions whose energy is on the order of kT, the thermal energy. These phonons scatter photons in the following two processes: A photon with momentum $\hbar\boldsymbol{q}_i$ absorbs one phonon with $\hbar\boldsymbol{k}$ to make a scattered photon with $\hbar\boldsymbol{q}_s$, conserving the momentum as $\hbar\boldsymbol{q}_i + \hbar\boldsymbol{k} = \hbar\boldsymbol{q}_s$; and a photon creates one phonon to make a scattered photon as $\hbar\boldsymbol{q}_i = \hbar\boldsymbol{q}_s + \hbar\boldsymbol{k}$. The energy conservation law increases or decreases the photon energy by $\hbar\omega$ in the former or latter process, which is referred to as anti-Stokes or Stokes scattering, respectively. Since $|\boldsymbol{q}_i| \cong |\boldsymbol{q}_s| = q$ is a very good approximation, the preceding two equations of momentum conservation are rewritten with the scattering angle Θ in scalar form as

$$2q \sin(\Theta/2) = k \tag{5}$$

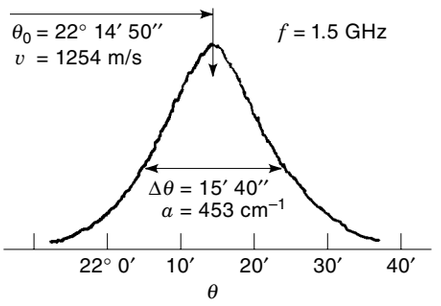

Figure 10. Typical curve of the HRB method, which is associated with the spectrum of k. The peak and width give the velocity and absorption, respectively. The sample is liquid CS_2.

In a classical description, Brillouin scattering is interpreted in terms of Bragg reflection by sound generated in thermal fluctuation. With $\Theta = 2\theta_B$, Eq. (5) agrees perfectly with the Bragg's condition of Eq. (2). The change in the phonon energy is understood as the Doppler shift. Figure 11 schematically shows the standard system of experiment. The incident laser is scattered by phonons in the specimen into all the solid angles, and a component with scattering angle Θ passes through the Fabry-Perot interferometer and is detected by a photomultiplier, which yields the power spectrum of the scattered light. The spectrum generally has three peaks, termed the Brillouin triplet. The central one is the Rayleigh component due to the slow diffusive decay of the spontaneous increase in temperature or density; the other two, symmetric with respect to the center, are Brillouin components of the Stokes and the anti-Stokes scattering, whose frequencies are shifted down and up by $\hbar\omega$, respectively. The shift gives ω, and Θ determines k with Eq. (5): Phonon velocity is obtained as $v = \omega/[2q \sin(\Theta/2)]$. The full width of the Brillouin peak $\delta\omega$ gives the lifetime of the phonon and hence the absorption: $\alpha = \delta\omega/2v$. The ratio of the intensity of the Rayleigh to the Brillouin component (named the Landau-Placzek ratio) is an important factor characterizing the thermodynamic property of the medium. The highest wave number of the phonon observed by Brillouin scattering is $2q$, which corresponds to 7 to 10 GHz in liquids and 50 GHz to 100 GHz in solids.

MOLECULAR ACOUSTICS

Sound propagation in fluids is strongly influenced by various phenomena of molecular origin, and measurement of the velocity and absorption provides an experimental approach to the microscopic structures and their dynamics. Velocity in liq-

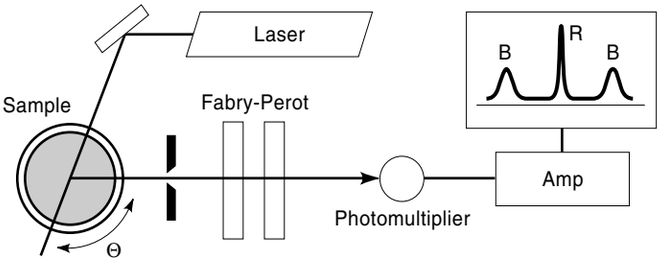

Figure 11. Basic system of Brillouin scattering experiment.

uid generally decreases with temperature since the elasticity decreases to a degree that exceeds the positive effect of decreasing density. The exception is water, which has a positive temperature gradient with a broad maximum at ~75°C. This anomaly is explained by the icelike clusters of associated molecules coexisting with monomers. An increase in temperature breaks these clusters, which have a lower elasticity than a collection of monomers, and increases the velocity. This effect is canceled at 75°C by the normal decrease.

A common mechanism of absorption in liquid is the viscous loss, referred to as classical absorption, which has f^2 dependence on frequency as

$$\alpha = (8\pi^2/3)(\eta f^2/\nu^3\rho) \tag{6}$$

where η is the viscosity. This equation includes the factor 4/3 for the shear strain component in the longitudinal vibration. Since α/f^2 is independent of f, this quantity is often used for characterizing the material. Most kinds of liquid have abosrption larger than the classical value, however, and the excess absorption is attributed to relaxation loss (17). Heat flow within one wavelength could be a loss mechanism at higher frequencies. However, sound propagation in the range of usual experiment is regarded as an adiabatic process: This absorption is safely ignored.

Ultrasonic Relaxation

A sudden increase in temperature, for example, disturbs the equilibrium of a system with some inner degrees of freedom, and the excess thermal energy is properly distributed among them with a finite time constant: The system gradually recovers balance through the relaxation process. Sound waves impart a periodic disturbance of temperature or pressure to the medium. If the period T is much greater than the relaxation time τ (time required for the recovery), the system always keeps its equilibrium. As T becomes shorter than τ, on the other hand, the system cannot follow the rapid alteration of sound and is brought into a nonequilibrium state with a constant strain. Some of the degrees of freedom freeze, losing their function as energy capacity. The medium apparently stiffens: The velocity increases and the absorption in α/f^2 decreases as the frequency increases through $f_r = 1/\tau$, the relaxation frequency. This is the general description of ultrasonic relaxation, and the velocity dispersion and absorption are expressed by the following equations:

$$v^2 = v_0^2 + (v_\infty^2 - v_0^2)/[1 + (f_r/f)^2] \tag{7}$$

$$\alpha/f^2 = A/[1 + (f/f_r)^2] + B \tag{8}$$

where v_0 and v_∞ are, respectively, the limiting velocities at lower and higher frequencies in the definition of relaxation strength, $\epsilon = (v_\infty^2 - v_0^2)/v_\infty^2$; $A = \pi\epsilon/(v_0 f_r)$ is a magnitude of the absorption change; and B is a constant representing the contribution of other relaxation mechanisms and the classical absorption. Besides v^2 and α/f^2, absorption per wavelength $\alpha'\lambda$ is also used for the discussion of relaxation, where $\alpha' = \alpha - Bf^2$ is the contribution of relaxation to absorption. The spectrum of $\alpha'\lambda$ has a bell shape with a maximum at f_r. Equations (7) and (8) are for a single relaxation process. If there are more than two relaxation mechanisms with different f_r and ϵ, dispersion and absorption are given by linear combinations of the relevant equations.

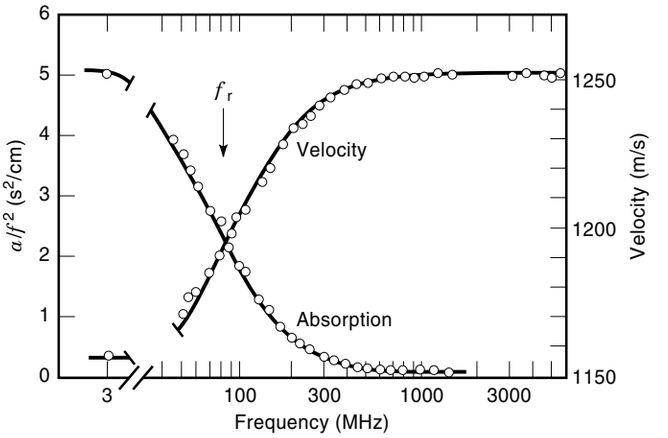

Figure 12. Strong velocity dispersion and anomalous absorption in liquid CS_2 are caused by the vibrational relaxation phenomenon.

For relaxation studies in liquid, ultrasonic spectroscopy, which observes v and α over a wide frequency range, is usually conducted. Since f_r is proportional to pressure in most cases of gas, the spectrum is obtained as varying P instead of f and is shown as a function of f/P. Temperature is often preferred as the variable in the study of solids.

Various Mechanisms of Relaxation

The most typical example of ultrasonic relaxation is observed in some kinds of polyatomic molecules, which have molecular vibration as the inner degrees of freedom. The vibration and translation motions of the molecules exchange energy through collisions. Analysis of vibrational relaxation is outlined in the following by considering the case of liquid carbondisulfide (CS_2) (18). Figure 12 shows the dispersion and absorption at 20°C observed by three techniques: the pulse method, HRB, and Brillouin scattering. The solid lines are the theoretical curves of Eqs. (7) and (8), which give $\epsilon = 0.15$, $f_r = 105$ MHz, and other parameters. This molecule has three independent modes of vibration—doubly degenerated deformation, symmetric stretching, and antisymmetric stretching—whose fundamental frequencies are at $\nu_1 = 397$ cm^{-1}, $\nu_2 = 658$ cm^{-1}, and $\nu_3 = 1540$ cm^{-1}, respectively. Each mode contributes to the specific heat in a static sense (at $f \leq f_r$), and the value is theoretically predicted by the equation of specific heat for a harmonic oscillator: $C_i = R\zeta_i^2 \exp \zeta_i/(\exp \zeta_i - 1)^2$, where $\zeta_i = h\nu_i/kT$. The contribution of all three modes is thus calculated to be $\Delta C = \Sigma C_i = 16.2$ J/mol · K (the effect of the degeneracy is taken into account). At $f \geq f_r$, however, the modes are assumed to lose the contribution and C_P decreases by this amount. Since the sound propagation is an adiabatic process, the decrease causes a dispersion whose magnitude is given by $\epsilon = (\gamma - 1)\Delta C/(C_P - \Delta C)$. This equation gives the theoretical value $\epsilon = 0.153$, which is in good agreement with the experimental value. This liquid has strong absorption in the megahertz range, which is ~10^3 times the value in water. The reason is that A is inversely proportional to f_r and that f_r is very low. Further, f_r is given by the product of the number of collisions per second and the probability of vibrational

excitation in a collision. The latter rapidly decreases as $h\nu$ exceeds kT, since such a high level can only be excited by a few rare molecules with speed much greater than the average. Even the lowest level is almost twice kT ($\sim$200 cm^{-1} at 20°C) in CS_2, and this is the intrinsic reason for the very slow relaxation at $\sim$100 MHz. Vibrational relaxation is observed in a few other liquids, including halogen derivatives of methane or cyclic compounds such as benzene or pyridine. These liquids have strong absorption in the megahertz range without exception.

Rotational isomers can also be a relaxation mechanism, in which the entropy difference between the isomers determines ϵ, and the energy barrier in between determines f_r. Other relaxation mechanisms include the hybrid association of molecules in alcohol-water mixtures, most chemical reactions in solutions, and the deformation of polymer chains (19). In many cases, the relaxation is not a single process, but is distributed in f_r. Dispersion extends over decades of frequency, as in polymer solutions.

ADVANCED TOPICS

Hyperresolution Phonon Spectroscopy

While Brillouin scattering is a very good means of phonon study, the experiment should be conducted with a sufficient resolution if qualitative discussion is to follow. A stable laser at its single-frequency oscillation is used as the light source. As for the spectrometer, the sophisticated system of tandem multipath Fabry-Perot gives the highest resolution of optical devices (20). It has two sets of scanning Fabry-Perot with different interorders, and the light is filtered three or five times through each of them. Computer control of the whole system is required for stable operation.

Electronic spectroscopy instead of the optical spectrometer can break through the limit of Fabry-Perot and yields a hyperresolution that is $\sim 10^3$ times as high depending on the phonon frequency (21). Figure 13 shows the optical heterodyne system for this purpose, in which the incident and the local oscillator light cross at Θ in the specimen. The local oscillator and the light scattered in the same direction take exactly the same path to a high-speed photodiode, which mixes them and generates beat current between them. A spectrum analyzer gives the phonon power spectrum. The frequency resolution is determined by the receiving bandwidth and can be increased up to 1 kHz, if necessary. Figure 14 shows two examples of a fine structure of the spectrum that can be attained by the hyperresolution. Figure 14(a) is half the Brillouin spectrum in liquid CS_2 with the very narrow and tall

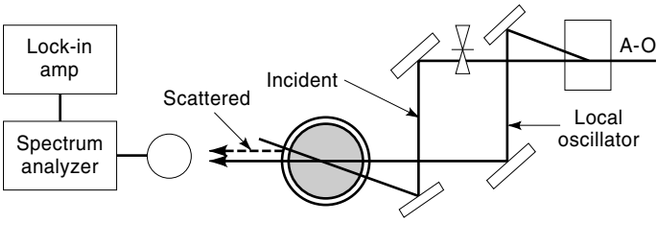

Figure 13. Hyperresolution Brillouin spectroscopy with the optical heterodyne technique.

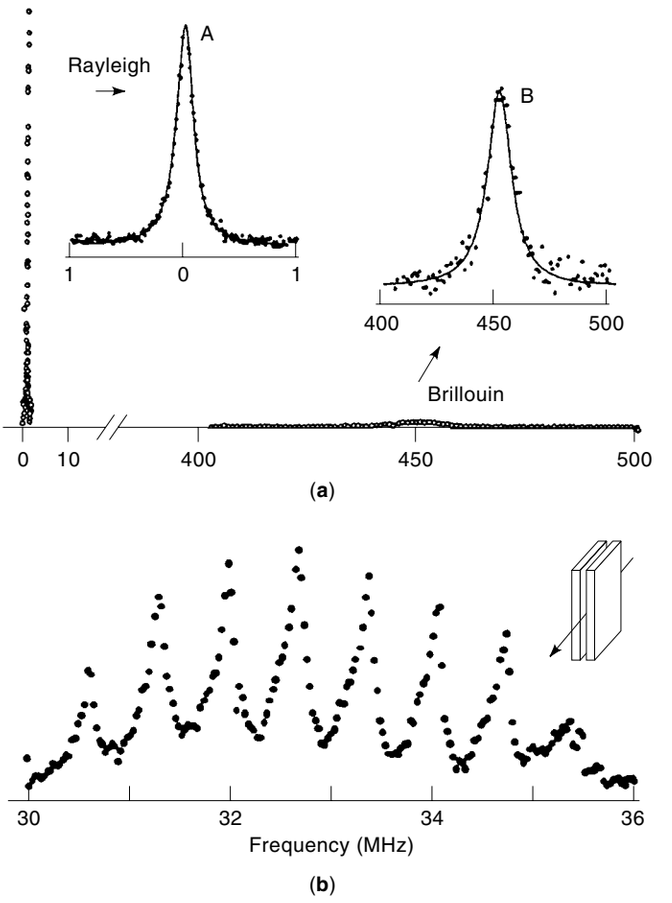

Figure 14. Two examples of phonon spectrum observed by the optical heterodyne technique. The real shape of the Brillouin spectrum is far from triplet, as shown in (a), where A and B are horizontal and vertical expansions of the Rayleigh and Brillouin components, respectively. Resonance of spontaneous phonons in a small cavity is observed in (b).

Rayleigh peak and the anti-Stokes Brillouin component, which is $\sim 10^2$ times broader and only $\sim 10^{-2}$ as high. Parts A and B show the expansion of $\sim 10^2$ along the abscissa and ordinate, respectively. Fabry-Perot with an instrumental width much broader than the Rayleigh line gives the more familiar curve known as the Brillouin triplet, though the real shape is far from triplet. Figure 14(b) is the Brillouin component obtained in a small cavity made of two glass plates $d = 900$ μm apart and filled with liquid toluene. Since a finite beam width of the laser introduces some ambiguity to Θ and hence to k, phonons with a certain range of ω are simultaneously observed. The spontaneous phonons in the cavity multiply reflect and resonate at an interval given by $v/(2d)$.

The optical spectrometer analyzes the phonon signal at $\sim 10^9$ Hz that is carried on a light wave with frequency $\sim 10^{15}$ Hz. Accuracy of 1% in phonon measurement requires a very severe resolution of $\sim 10^{-8}$. In electronic spectroscopy, on the other hand, the optical mixing demodulates the carrier light to give the bare phonon signal whose frequency is in the range easily treated by a spectrum analyzer. This is the intrinsic difference yielding hyperresolution.

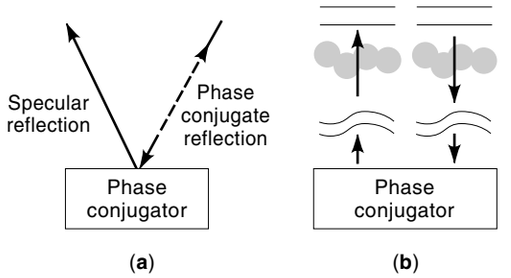

Figure 15. Time-reversal property of phase conjugate waves (a), and the function to correct the wavefront distortion automatically (b).

Acoustic Phase Conjugate Waves

Given a wave expressed by a complex function $\phi(\boldsymbol{r}, t) \exp(-j\omega t)$, the phase conjugate wave of the wave is defined as $\phi^*(\boldsymbol{r}, t) \exp(-j\omega t)$, where $\boldsymbol{r}$ is a position vector and the asterisk means the complex conjugate. Their amplitudes are written in a scalar form as $U(\boldsymbol{r}, t)$ and $U(\boldsymbol{r}, -t)$. The latter has the same spatial distribution as the former but advances in the opposite direction. A phase conjugator (or a phase conjugate mirror) is a device that generates the time reversal of the incident wave and has a function to automatically correct the wavefront distortion suffered along the path, as shown in Fig. 15. This phenomenon offers potential applications such as in imaging systems and is studied in the fields of optics and acoustics. Of the different principles of ultrasonic phase conjugation, nonlinear piezoelectricity provides sufficient efficiency, fidelity, and high-speed response (22). The phase conjugator is made of a PZT ceramic block with two electrodes. The ultrasonic pulse at ω ($\sim$10 MHz) is incident on the top surface 5×10 mm in size and a high electric field at 2ω is simultaneously applied between the 10×50 mm side faces. The nonlinear interaction then occurs between the ultrasonic and electric field, and the crossterm yields a component of $-\omega t$ ($= \omega t - 2\omega t$), which returns as the phase conjugate pulse. In addition to piezoelectricity, nonlinearity in the elastic or dielectric constant is part of the effect, though the contribution is smaller. Slow-motion video taken by the Schlieren technique visually confirms the time reversal property of the phase conjugate propagation in water. Figure 16 shows the three shots of the video: (a) A focused incident pulse has just arrived at the PZT surface and (b) is specularly reflected, and (c) the phase conjugate appears after a few microseconds.

The phase conjugator was installed as a reflector in an imaging system operating at 10 MHz, which is essentially the same as the scanning acoustic microscope. The target to be imaged is a thin metal plate with letter-shaped holes and put in agarose gel with a very irregular shape. The sound velocity of the agarose gel is $\sim$15% higher than the surrounding water, and its rough surface distorts the ultrasonic wavefront. The normal and phase conjugate images were taken without and with the 2ω electric field and are compared in Figs. 17(a) and 17(b), respectively. Phase conjugate imaging is useful in observing the inner part of something whose velocity is not uniform, like a biological specimen, or of a specimen whose surface is not flat.

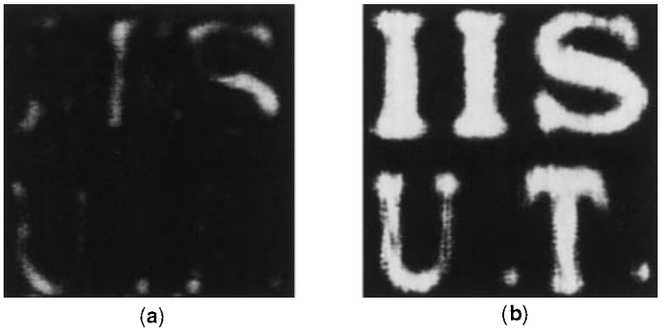

Figure 17. Comparison of images reconstructed by a scanning acoustic system (a) without and (b) with the phase conjugator. The target is put in agarose gel with an irregular shape, which disturbs the wavefront. The ultrasonic frequency is at 10 MHz and the letters have 3.5 mm height.

Other principles of acoustic phase conjugation are magnetostriction, liquid surface holography, and nonlinear oscillation of air bubbles in water, though the latter two lack stability and a real-time response and are not suitable for the purpose of imaging.

Laser-induced Ultrasound

The photoacoustic effect is applied for the purpose of noncontact ultrasonic generation in gas, liquid, and solids, and many varieties of techniques are being studied, as shown in Fig. 18. A giant Q-switched laser pulse strikes a metal surface in Fig. 18(a) and the sudden heating of a small area excites elastic vibration, which propagates into all the possible directions as SAW and bulk waves of both longitudinal and transverse modes (23). The frequency has a distribution depending on the sharpness of the laser pulse. The conversion efficiency is rather low, but the laser power should be kept below a certain level for fear of surface ablation and damage. The lack in the

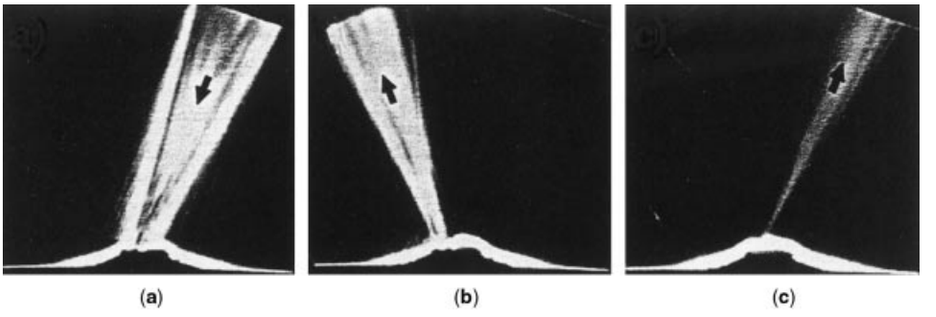

Figure 16. The time-reversal property is visually shown by the storoboscopic Shlieren technique: (a) focused incidence at $t = 0$, (b) specular reflection at $t = 7$ μs, and (c) phase conjugate reflection at $t = 15$ μs.

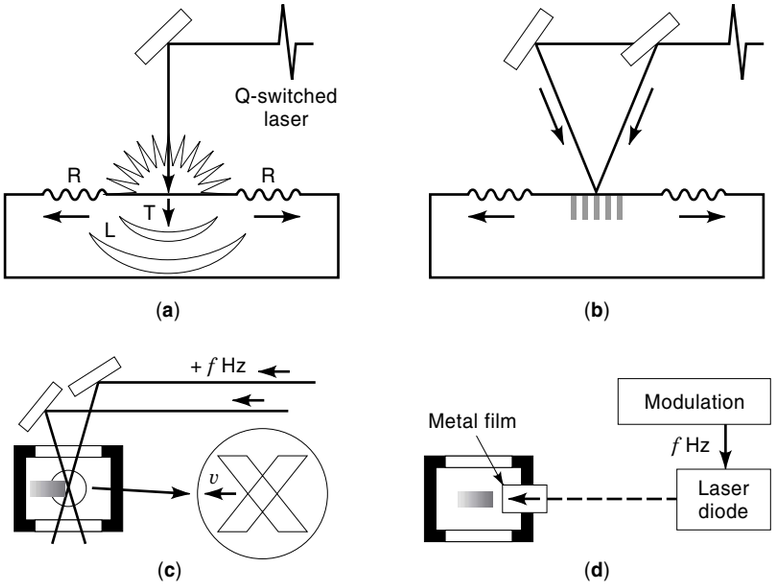

Figure 18. Various mechanisms of laser-induced ultrasound: (a) A giant pulse laser strikes the surface to generate both surface acoustic waves (SAW) and bulk waves; (b) two beams crossing at the surface project a fringe that generates SAW; (c) running standing waves of electric field made by two beams with different frequencies effectively generate ultrasound in liquid; and (d) sinusoidally modulated output of infrared laser generates ultrasound on the metal film.

efficiency, mode selectivity, directivity, and wave coherence is improved in Fig. 18(b). Two laser pulses irradiate the same area from different directions and instantaneously project a fringe pattern whose interval Λ is determined by the crossing angle Θ as $\Lambda = \pi/(q \sin \Theta/2)$. The plane SAW with wavelength Λ is selectively excited and propagates in the direction normal to the fringe. The efficiency is further increased by an acousto-optic modulator, which gives a frequency difference of f between the two pulses. The fringe runs on the surface at a speed of $f\Lambda$ and efficiently excites SAW when the speed agrees with the phase velocity. Since most of the SAW generations aims at noncontact ultrasonic evaluation (for example, of very hot plates for which piezoelectric transducers are of no use), noncontact detection is also essential. A laser probe provides remote sensing of the waves in the optical lever or interferometer.

Figure 18(c) shows bulk wave generation at ~3 GHz in a transparent liquid based on the same principle as the cross-beam method, but with two CW lasers whose frequency can be swept by means of thermal control. In the absence of optical absorption, the electrostrictive effect is the origin of photoacoustic coupling. A simple yet effective method is shown in Fig. 18(d) that utilizes a CW semiconductor laser. The infrared output is electrically modulated at f and irradiates a thin metal film evaporated on a fused quartz rod, which works as the ultrasonic transducer with an even frequency response. The signal can be detected by Brillouin scattering, as shown in Fig. 19. The phonon density is $\sim 10^4$ times as high as the spontaneous phonons excited by kT.

The most remarkable example of sound-and-light interaction can be seen in the phenomenon of stimulated Brillouin scattering. A giant-pulse laser induces a coherent beam of phonons in a transparent medium, and the phonon beam, in turn, reflects the laser in a backward direction. Thus photoacoustics and acousto-optics occur simultaneously.

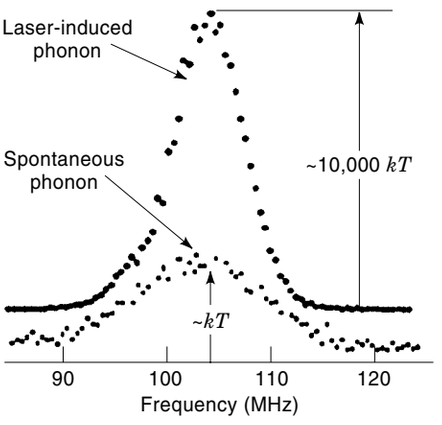

Figure 19. Coherent phonons generated by the method (d) in Fig. 18 have $\sim 10^4$ as large population as the spontaneous phonons.

BIBLIOGRAPHY

1. R. B. Lindsay, The story of acoustics, *J. Acoust. Soc. Amer.,* **39** (4): 629–644, 1966.
2. H. F. Pollard, *Sound Waves in Solids,* London: Pion, 1977.
3. L. A. Victorov, *Rayleigh and Lamb Waves,* New York: Plenum, 1967.
4. D. Berlincourt, R. Curran, and H. Jaffe, Piezoelectric and piezomagnetic materials and their function in transducers. In W. P. Mason (ed.), *Physical Acoustics,* Vol. 1A, New York: Academic, 1964.
5. F. S. Foster, *Handbook of Thin Film Technology,* Chap. 5, New York: McGraw-Hill, 1970.
6. C. Kittel, *Introduction to Solid State Physics,* 3rd ed., New York: Wiley, 1966.
7. J. M. Ziman, *Electrons and Phonons,* Oxford: Clarendon, 1960.
8. S. Tamura, J. A. Shields, and J. P. Wolfe, Lattice dynamics and elastic phonon scattering in silicon, *Physical Rev. B,* **44**: 3001–3011, 1991.
9. J. Sapriel, *Acousto-Optics,* New York: Wiley, 1979.

10. A. McDonald and G. C. Westel, Jr., Theory of photothermal and photoacoustic effects in condensed matter. In W. P. Mason and R. N. Thurston (eds.), *Physical Acoustics,* Vol. XVIII, New York: Academic, 1988.
11. L. A. Crum, Sonoluminescence, *Physics Today,* **9**: 22–29, 1994.
12. K. Negishi, Visualization of ultrasonic pulse in glass by the technique of photoelasticity, *Japanese J. Appl. Physics,* **22** (3): 19–21, 1983.
13. E. Papadakis, Ultrasonic velocity and attenuation: Measurement methods with scientific and industrial applications. In W. P. Mason and R. N. Thurston (eds.), *Physical Acoustics,* Vol. VII, New York: Academic, 1970.
14. D. I. Bolef and J. G. Mirror, High-frequency continuous wave ultrasonics. In W. P. Mason and R. N. Thurston (eds.), *Physical Acoustics,* Vol. VIII, New York: Academic, 1971.
15. K. Takagi and K. Negishi, Measurement of ultrasonic velocity and absorption in liquids up to 1.5 GHz by the high-resolution Bragg reflection technique, *J. Phys., D,* **15**: 757–765, 1982.
16. P. A. Fleury, Light scattering as a probe of phonons and other excitation. In W. P. Mason and R. N. Thurston (eds.), *Physical Acoustics,* Vol. VI, New York: Academic, 1970.
17. K. F. Hertzfeld and T. A. Litovitz, *Absorption and Dispersion of Ultrasonic Waves,* New York: Academic, 1959.
18. K. Takagi, Vibrational relaxation in liquid carbondisulfide, *J. Acoust. Soc. Amer.,* **71** (1): 74–77, 1982.
19. A. J. Matheson, *Molecular Acoustics,* London: Wiley-Interscience, 1971.
20. J. R. Sandercock, Light scattering in solids III. In M. Cardona and G. Cruntherodt (eds.), *Topics in Applied Physics,* Berlin: Springer, 1982.
21. T. Matsuoka, K. Sakai, and K. Takagi, Hyper-resolution Brillouin-Rayleigh spectroscopy with an optical beating technique, *Rev. Sci. Instrum.,* **64** (8): 2136–2139, 1993.
22. K. Yamamoto et al., Nonlinear piezoelectricity of PZT ceramics and acoustic phase conjugate waves, *Japanese J. Appl. Phys.,* **35** (5B): 3210–3213, 1996.
23. D. A. Hutchins, Ultrasonic generation by pulsed laser. In W. P. Mason and R. N. Thurston (eds.), *Physical Acoustics,* Vol. XVIII, New York: Academic, 1988.

KENSHIRO TAKAGI
University of Tokyo

PHYSICAL MECHANISMS AND CHEMICAL EFFECTS OF ULTRASOUND.

See ULTRASONIC PHYSICAL MECHANISMS AND CHEMICAL EFFECTS.